Appl. Phys. B 79, 139–143 (2004)
DOI: 10.1007/s00340-004-1545-z

Applied Physics B
Lasers and Optics

Rapid communication

V. SICK✉
N. WERMUTH

Single-shot imaging of OH radicals and simultaneous OH radical/acetone imaging with a tunable Nd : YAG laser

Department of Mechanical Engineering, The University of Michigan,
2023 W.E. Lay Automotive Laboratory, 1231 Beal Ave., Ann Arbor, MI 48109-2133, USA

Received: 25 February 2004/Revised version: 22 April 2004
Published online: 20 May 2004 • **© Springer-Verlag 2004**

ABSTRACT Single shot imaging capability for OH radical distributions in various atmospheric pressure methane flames upon excitation with a tunable frequency-quadrupled Nd : YAG laser is demonstrated. The laser wavelength can be tuned with an intra-cavity etalon to produce laser-induced fluorescence (LIF) signals from OH via absorption in the OH A–X (2,0) $P_1(10)$ line. Simultaneous single-shot imaging of the burnt and unburnt zones in laminar nonpremixed, premixed and turbulent flames is presented. The unburnt areas are visualized with LIF of acetone that is seeded to the methane fuel. Acetone levels are set to match signal intensities to that of the OH signals to allow imaging on a single intensified CCD camera.

PACS 42.62.Fi; 33.50.Dq; 82.33.Vx

1 Introduction

Measurements of the hydroxyl radical (OH) have been attractive for countless combustion studies. Formed in the flame front and still present in hot exhaust gases, OH radicals can be used as flame-front markers with reasonable accuracy – although correlations with heat release might be problematic. The strength of the A–X transitions and the magnitude of the vibrational and rotational constants made this radical a simple target for sensitive and selective laser-based diagnostic techniques [1]. Amongst the approaches used for OH measurements are absorption-based techniques as well as laser-induced fluorescence (LIF). LIF measurements can be performed with laser light sheets and intensified cameras; thereby planar images of the species under study are obtained. Due to the strength of the OH transitions, OH was amongst the first molecules for which planar LIF images were obtained [2, 3]. Excitation and detection for OH LIF measurements has been demonstrated for a wide range of combinations. Ketterle et al. [4] compared different excitation/detection schemes that can be realized with tunable excimer lasers and compared these to excitation with tunable dye lasers. Excitation within the strongest band, the A–X (0,0) band near 310 nm, requires detection of LIF signals in the same band. Separation of scattered light from surfaces or droplets is difficult then. However, applications to internal combustion engines are reported [5]. Detection of the (0,1) band after (0,0) excitation yields weaker signals but still of measurable intensity [4] and with the advantage that scattered light is now suppressed. Excitation within the (3,0) band with a tunable KrF excimer laser, first demonstrated by Andresen et al. [6], produces signals that can be detected nearly quench free due to the predissociative nature of the OH A, $v' = 3$ state. However, there is the risk that high pulse energies lead to temporary ground-state depletion, which makes quantitative measurements problematic [7, 8]. Also, for highest signal yield, all of the LIF signals that are emitted from lower vibrational states after they were populated from $v' = 3$ via efficient vibrational energy transfer are often detected. Thus, quenching does influence the measured signals. Many studies that are published in the literature use tunable dye lasers (or, more recently, optical parametric oscillator systems) to excite OH within the (1,0) band near 280 nm and then signals are detected from the (1,1) and (0,0) bands near 310 nm. This allows effective suppression of scattered light and, while still providing sufficient signal levels at approximately 2.5% of that which can be achieved with a tunable excimer laser at 308 nm, it is a scheme that works very well. The abundance of OH radicals and large absorption cross sections for the (0,0) band sometimes bias LIF measurements because both the exciting laser beam and the signals are attenuated strongly. Excitation in the (1,0) band suffers less from this problem.

In this paper we report an excitation scheme that uses light from a tunable, frequency-quadrupled Nd : YAG laser for excitation of OH in the (2,0) band. We discuss details of the transitions and compare the signal strength to other schemes and demonstrate single shot imaging capability with this system. It is also demonstrated that acetone, which is a popular fluorescence tracer for mixing experiments, can be imaged simultaneously with OH radicals upon excitation with the same laser pulse. Images of the two species can be recorded on the same intensified CCD camera. Previous measurements to simultaneously detect OH and acetone used excitation

✉ Fax: +1-734/764-4256, E-mail: vsick@umich.edu

in the OH (0,0) band with XeCl lasers at 308 nm by Yip et al. [9] and dye lasers in the (1,0) band by Seitzman et al. [10]. Similarly, the simultaneous detection of OH and 3-pentanone was used in engine studies by Arnold et al. [11] using a KrF excimer laser (248 nm) to excite OH in the (3,0) band and a XeCl excimer laser (308 nm) for 3-pentanone and by Rothamer and Ghandhi [12], who used a dye laser to excite 3-pentanone and OH in the (1,0) band.

2 Experiment

A LIF experiment was set up to detect laser-induced fluorescence from OH radicals and/or acetone in either imaging or dispersion mode. Normal to the laser beam a combination of two achromatic UV lenses (OptoSigma, diameter = 47 mm, $f = 50$ mm and $f = 250$ mm, respectively) collected fluorescence signals to focus them on to the slit of a spectrometer (ARC 150). The spectrometer was equipped with a 1200-l/mm grating that was blazed for 300 nm. Dispersed LIF signals were detected with a combination of an image intensifier (LaVision IRO) and a CCD camera (LaVision FlowMaster 3S) that were coupled to each other. The intensifier gate width was set to 200 ns to completely suppress any luminosity from the flames as well as artificial lighting in the laboratory. The pixel resolution of the spectrometer/camera combination is 0.0677 nm/pixel. Alternatively, the image intensified camera system was equipped with a UV lens (Nikor 105 mm, $f_{\#} = 4.5$) and a Schott glass filter (WG280) to record OH and acetone LIF images.

OH radicals were excited in the A–X (2,0) band using a tunable Nd : YAG laser (LaVision T-YAG). This laser can be tuned with an intra-cavity etalon to lase on the sideband that is usually suppressed in typical Nd : YAG lasers as shown in Fig. 1. Rayleigh scattering signals in air were recorded to measure the output of the laser for a range of etalon angles. It has to be noted that the frequency-quadrupling crystal should be tuned as well to maintain peak pulse energies while changing the etalon angle. This has not been done for the spectrum shown in Fig. 2. Also, since the gain curve of the Nd : YAG material is not continuous over the range shown, rather consisting of two more or less separated peaks (as illustrated in Fig. 1), the spectral composition in the center of the tuning range should actually be analyzed in more detail. However, once the etalon forces the laser to run in the sideband, the laser wavelength can be fine tuned to be coincident with the A–X (2,0) $P_1(10)$ transition at 266.188 nm [13]. The spectral width of the laser fundamental without etalon is 1.0 cm^{-1} [14]; frequency quadrupling will increase this bandwidth to approximately 2 cm^{-1} at 266 nm. The etalon reduces this bandwidth to 0.47 cm^{-1} at the fundamental wavelength and approximately 0.94 cm^{-1} at 266 nm.

With pulse energies of up to 50 mJ for our laser, light sheets of several cm height can be used for OH imaging experiments. Acetone absorbs 266-nm light and subsequently emits fluorescence in the range of ∼ 350–550 nm; for details see Thurber and Hanson [15]. The absorption spectrum of acetone has no resolved rotational structure at 266 nm and, thus, tuning of the Nd : YAG laser will affect only the OH

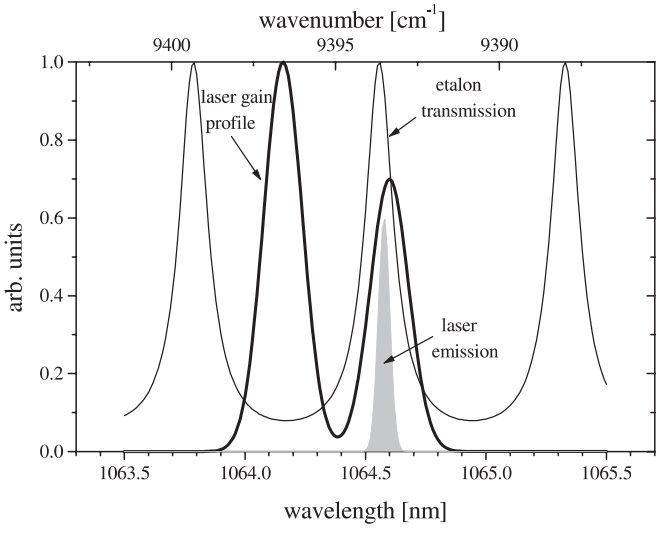

FIGURE 1 Schematic illustration of the laser gain curve and etalon transmission tuned to force the laser output to the sideband (courtesy of T. Berg [23])

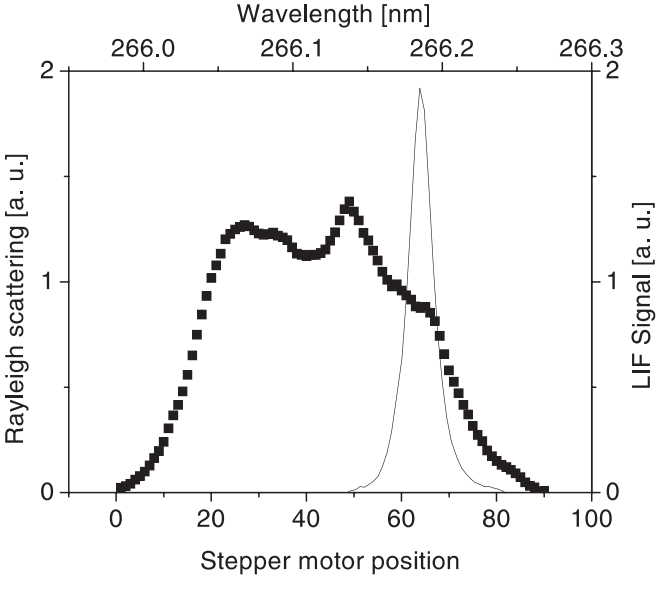

FIGURE 2 Laser output as measured via Rayleigh scattering (■) and LIF signals (–) measured at wavelengths higher than 270 nm. Note that the wavelength scale is given to illustrate the position of the OH line but should not be taken as an indication that the laser can be tuned continuously (Fig. 1). Also, the tuning of the quadrupling crystal was not adjusted to maximize the output for each stepper-motor position

radical excitation. After excitation in the (2,0) band, the OH radical fluorescence is emitted in the range of ~ 265–325 nm and, thus, it can be spectrally separated from acetone fluorescence and recorded on a different camera. An image-splitting technique could also be used to record the two signals simultaneously on a single camera [16]. As will be shown below, the spatial separation of the OH and acetone LIF signals is sufficient to image both signals directly on a single camera.

OH radicals were generated in atmospheric pressure methane flames on a small laboratory Bunsen burner with a nozzle diameter of 11 mm. The settings of the burner were chosen such that nonpremixed as well as premixed flames of various flow conditions could be established to demonstrate the performance of the OH imaging scheme. Acetone was added to the methane flow by bubbling a portion of the methane through liquid acetone at room temperature and then introducing this stream into the main methane flow. The amount of acetone was adjusted such that the acetone LIF signals were comparable in strength to the OH signals.

3 Results

The etalon was tilted while monitoring wavelength-dispersed signals. Figure 2 displays Rayleigh scattering signals measured in ambient air and LIF signals measured in the exhaust gases of a premixed Bunsen flame. At a laser wavelength of 266.188 nm (quadrupled) the OH $P_1(10)$ transition absorbs and subsequently LIF signals were observed from several bands near 265, 290 and 310 nm as shown in Fig. 3.

The $v' = 2$ levels are predissociative and the radiative lifetime of $N' = 9$ into which the excitation leads is shortened from ~ 871 ns to approximately 30 ns [13]. With quenching lifetimes for A-state levels on the order of 1–2 ns [17–19] and rotational and vibrational energy transfer rates [18, 20, 21] high enough to allow some redistribution of the original excited-state population a substantial fraction of the excited molecules radiate from levels other than $N' = 9$. So, while a prominent portion of the emission spectrum is given by transitions starting from $N' = 9$ ($P_1(10)$, $Q_1(9)$ and $R_1(8)$) for the (2,0), (2,1) and (2,2) bands, more rotational scrambling is observed for transitions that originate from $v' = 1$ and $v' = 0$ since the rotational quantum number is not preserved during vibrational energy transfer.

Even though the radiative lifetime is reduced by predissociation to ~ 30 ns, the fluorescence quantum yield is only modestly affected by this. Assuming a quenching lifetime of 2 ns (as for other A-state vibrational levels) the fluorescence quantum yield is dominated by quenching. An approximate signal strength analysis following the comparison given in Table 1 of Ketterle et al. [4] for other OH transitions yields expected LIF signals for (2,0) excitation that are comparable to those achieved with tunable dye lasers when exciting in the (1,0) band. The dominant contribution to the OH line width is Doppler broadening in atmospheric pressure flames, ranging from 0.21 cm^{-1} at 1000 K to 0.33 cm^{-1} at 2500 K. The lifetime broadening due to predissociation is negligible; pressure broadening contributes by approximately 0.06 cm^{-1}/bar. The convolution with the laser emission profile (width at 266 nm ~ 0.94 cm^{-1}) yields a nondimensional overlap integral [22] that changes less than 4% from 1000 K to 2500 K. The excitation with the tunable Nd : YAG laser starts from $N'' = 10$ and Fig. 4 illustrates the thermal population of this level to demonstrate the reduced temperature sensitivity of the detection scheme. However, the signal strength analysis will have to include temperature and composition dependence of fluorescence quenching [19] as in other OH LIF measurement strategies.

The following images demonstrate the single-shot capability of the OH radical imaging approach with a tunable Nd : YAG laser as well as illustrate the

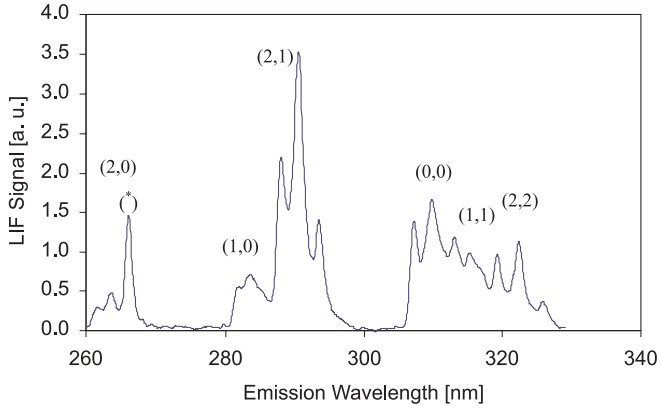

FIGURE 3 Fluorescence spectrum of OH radicals after excitation at 266.188 nm, the $P_1(10)$ transition in the A–X (2,0) band. The OH vibrational bands are indicated in parentheses (v',v''). The stronger peak near 266 nm (*) is Rayleigh scattering since this spectrum was recorded in relatively cool exhaust gas regions of a flame

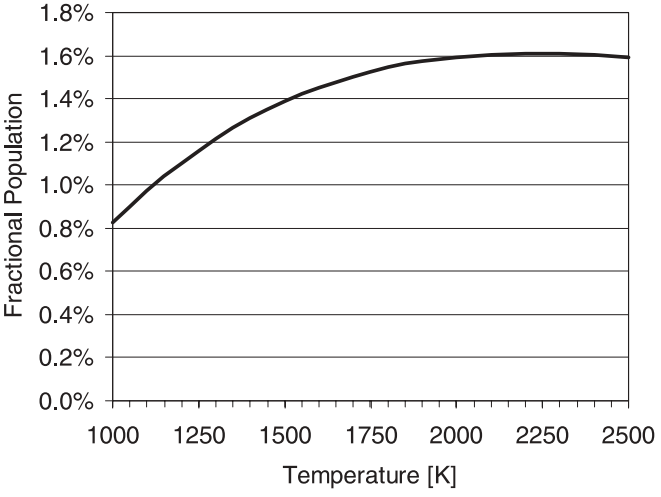

FIGURE 4 Fractional population of $N'' = 10$ level from which the $P_1(10)$ transition starts

possibility of simultaneously obtaining fuel distribution data through LIF imaging of acetone. No attempt was made at calibrating the signals to absolute concentrations for the purpose of this study. As such, none of the presented images were corrected for laser pulse energy and the intensity distribution across the light sheet. Laser-sheet dimensions were approximately 50 mm × 0.5 mm at the flame location. With typical pulse energies of 10 mJ within approximately 3 ns, power densities on the order of 13 MW/cm^2 were achieved. Figure 5 displays two examples of single-shot OH distributions measured in laminar nonpremixed and premixed flames, respectively. While OH is found only at the interface between air and fuel in the nonpremixed flame, in a premixed flame OH is present right at the flame front of the inner premixed flame; unburnt fuel from this flame burns as a nonpremixed flame on the outside of this cone. This structural change is clearly visible in the images of Fig. 5.

Tuning the laser off-resonant with the OH transition will result in nonmeasurable signals for the premixed flames; in nonpremixed flames signals of up to 5% of that of the peak OH signal could be measured on the fuel side of the OH distribution. As will be shown below, this signal is due to intermediates that are formed in the flame front.

Once acetone was added to the methane stream, additional LIF signals were observed. Single-shot examples that were recorded with the Nd : YAG laser tuned to the OH transition are displayed in Fig. 6. The OH structure is as already seen in Fig. 5 and in the inner cone, where the fuel is emerging from the Bunsen burner nozzle, acetone LIF signals are recorded.

A faint line of signal between the OH and the fuel zone is barely noticeable for the nonpremixed flame. This again is due to intermediates and is at a level of no more than 5% of the OH signal. This signal remains when the laser is tuned away from the OH transition. No such signal is observed in premixed flames as the one shown in the right-hand panel of Fig. 6. A comparison of images taken on- and off-resonant with the OH transition excitation line for a more turbulent premixed Bunsen flame is presented in Fig. 7.

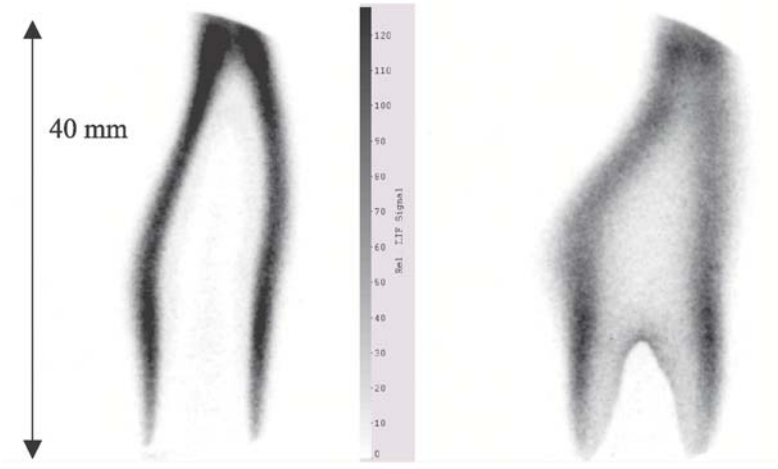

FIGURE 5 Single-shot OH images taken in laminar methane/air flames that were stabilized on a laboratory Bunsen burner. The *left-hand image* is from a nonpremixed flame; the *right-hand image* was recorded in a premixed flame. The distinct difference in the OH distribution is clearly recognizable

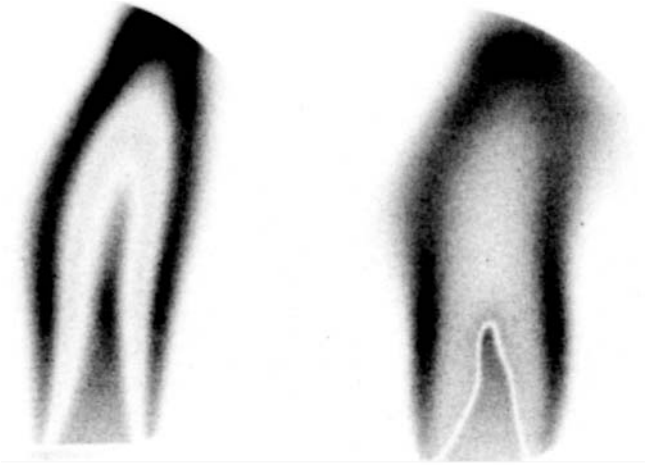

FIGURE 6 Simultaneously recorded single-shot distributions of OH radicals and acetone in laminar methane/air flames. The *left-hand image* shows a large gap between the fuel, represented by the acetone LIF signals in the inner cone, and the OH radicals that are found in the diffusion zone of the flame. The *right-hand image* was acquired in a premixed methane/air flame. The gap between the fuel and OH distribution in the premixed portion of the Bunsen flame is significantly smaller than that seen in the diffusion flame on the *left*

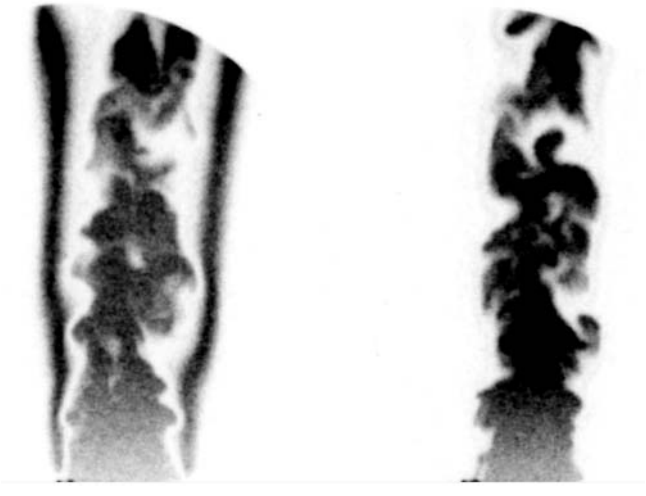

FIGURE 7 Example of single-shot imaging in a more turbulent Bunsen flame. The *left-hand image* shows the combined OH and acetone LIF signals. The highly wrinkled acetone (fuel) distribution is surrounded by a smooth layer of OH radicals. For the *right-hand image* the laser was tuned away from the OH line and thus only acetone signals are produced

In this case, faint signals are observed in some locations outside of the areas where OH or fuel are found. These signals follow more closely the outline of the highly wrinkled fuel distribution and not the smooth OH distribution that surrounds the fuel stream towards the surrounding air. When the WG280 filter is replaced with a WG365 filter that has a cutoff wavelength of 365 nm, the signals that are attributed to flame intermediates completely disappear in almost all cases. It is known that polycyclic aromatic hydrocarbons, which are formed as intermediates in hydrocarbon flames even for fuels like methane, absorb light in the UV and emit LIF signals in the range of $\sim$ 250–350 nm or even longer for very large molecules.

4 Conclusions

Single-shot imaging of OH radical distributions was demonstrated with a tunable, frequency-quadrupled Nd : YAG laser. This provides a convenient, simple and robust source for specific excitation of OH radicals. The $P_1(10)$ transition in the A–X (2,0) band could be excited to produce LIF signals of comparable strength to those obtained with frequently used excitation schemes using the (1,0) band. Nonresonant fluorescence background signals are below 5% for nonpremixed methane/air flames and not significant for premixed methane/air flames. It was further demonstrated that it is possible to simultaneously excite acetone and image the LIF signals from acetone onto the same camera. Simultaneous imaging on one camera, however, will only work if the spatial structure of the flame is known and there is no ambiguity as to where fuel and OH radicals should be located. In the case where turbulent mixing has produced a mixing pattern as in a direct-injection engine, it is not possible to assign signals to OH or acetone based on where the signal occurs. In such cases, spectral and subsequently spatial signal separation is required. The same strategy for simultaneous imaging of OH and acetone will work for imaging of OH and other ketones, such as the widely used 3-pentanone.

ACKNOWLEDGEMENTS This work was sponsored by General Motors Corporation through the General Motors–University of Michigan Collaborative Research Laboratory on Engine Systems Research. NW was supported by a postdoctoral fellowship from Deutsche Forschungsgemeinschaft. The authors would also like to acknowledge helpful discussions with T. Berg.

REFERENCES

1 K. Kohse-Höinghaus, J.B. Jeffries (eds.): *Applied Combustion Diagnostics* (Taylor and Francis, New York 2002)
2 G. Kychakoff, R.D. Howe, R.K. Hanson, J.C. McDaniel: Appl. Opt. **21**, 3225 (1982)
3 M.J. Dyer, D.R. Crosley: Opt. Lett. **7**, 382 (1982)
4 W. Ketterle, M. Schäfer, A. Arnold, J. Wolfrum: Appl. Phys. B **54**, 109 (1992)
5 R. Suntz, H. Becker, P. Monkhouse, J. Wolfrum: Appl. Phys. B **47**, 287 (1988)
6 P. Andresen, A. Bath, W. Groger, H.W. Lulf, G. Meijer, J.J. t. Meulen: Appl. Opt. **27**, 365 (1988)
7 J.W. Daily, E.W. Rothe: Appl. Phys. B **68**, 131 (1999)
8 E.W. Rothe, Y. Gu, A. Chryssostomou, P. Andresen, F. Bormann: Appl. Phys. B **66**, 251 (1998)
9 B. Yip, M.F. Miller, A. Lozano, R.K. Hanson: Exp. Fluids **17**, 330 (1994)
10 J.M. Seitzman, M.F. Miller, T.C. Island, R.K. Hanson: Proc. Combust. Inst. **25**, 1743 (1994)
11 A. Arnold, A. Buschmann, B. Cousyn, M. Decker, V. Sick, F. Vannobel, J. Wolfrum: SAE Trans. **102**, 1 (1993)
12 D.A. Rothamer, J.B. Ghandhi: SAE Tech. Pap. Ser. 2003-01-0069 (2003)
13 J. Luque, D.R. Crosley: *LIFBASE*, v2.0.2 edn. (SRI International, Menlo Park, CA, USA 1999) [MP-99-0099; http://www.sri.com/psd/lifbase]
14 Continuum: *Surelite Laser Manual* (2000)
15 M. Thurber, R.K. Hanson: Appl. Phys. B **69**, 229 (1999)
16 B.D. Stojkovic, V. Sick: Appl. Phys. B **73**, 75 (2001)
17 R. Schwarzwald, P. Monkhouse, J. Wolfrum: Proc. Combust. Inst. **22**, 1413 (1988)
18 F. Bormann, T. Nielsen, M. Burrows, P. Andresen: Appl. Opt. **36**, 6129 (1997)
19 P.H. Paul: J. Quantum Spectrosc. Radiat. Transfer **51**, 511 (1994)
20 A. Brockhinke, W. Kreutner, U. Rahmann, K. Kohse-Hoinghaus, T.B. Settersen, M.A. Linne: Appl. Phys. B **69**, 477 (1999)
21 T. Nielsen, F. Bormann, M. Burrows, P. Andresen: Appl. Opt. **30**, 7960 (1997)
22 W.P.J. Partridge, N.M. Laurendeau: Appl. Opt. **34**, 2645 (1995)
23 T. Berg: LaVision GmbH, private communication (2004)